




Düzce University Journal of Science & Technology

Research Article

Numerical Modeling of the Sound Generated on an Intracranial Aneurysm Using Computational Fluid Dynamics

 Hüseyin Enes SALMAN^{a,*}

^a Makine Mühendisliği Bölümü, Mühendislik Fakültesi, TOBB Ekonomi ve Teknoloji Üniversitesi, Ankara, TÜRKİYE

* Sorumlu yazarın e-posta adresi: hsalman@etu.edu.tr
DOI: 10.29130/dubited.1061673

ABSTRACT

An intracranial aneurysm is the enlargement of an artery in the brain which may lead to rupture and result in serious health disorders. The exact mechanism of aneurysm formation is still unclear; however, the disturbed hemodynamics take part in the initiation of the vessel enlargement. In this study, a simplified intracranial aneurysm is numerically investigated to elucidate the disturbed flow conditions and the generated sound on the aneurysm wall. For determining the generated sound, the pressure fluctuations on the inner wall are obtained using computational fluid dynamics simulations. Large eddy simulation model is employed to find the unsteady flow pressures. The results indicate that the sound levels increase at the proximity of the intracranial aneurysm. The sound levels on the aneurysm are compared to the sound levels on the sites with normal vessel diameter, and it is seen that the aneurysm results in about a 10 dB increase in the sound generation. This relative increase in the flow-generated sound is important in terms of the diagnosis of the intracranial aneurysms, which can be used as a diagnostic tool for the early detection of the aneurysm before facing serious symptoms.

Keywords: Acoustic pressure, Computational fluid dynamics, Hemodynamics, Intracranial aneurysm

İntrakraniyal Anevrizma Üzerinde Oluşan Sesin Hesaplamalı Akışkanlar Dinamiği Kullanılarak Sayısal Modellenmesi

ÖZ

İntrakraniyal anevrizma, beyindeki bir arterin yırtılmasına ve ciddi sağlık bozukluklarına yol açabilecek bir damar genişlemesidir. Anevrizma oluşumunun kesin nedenleri hala belirsizdir; ancak bozulmuş hemodinamik parametreler ve kan akış koşullarındaki anormallikler damar genişlemesinin başlamasında rol oynar. Bu çalışmada, bozulmuş akış koşullarını ve anevrizma duvarında oluşan sesi incelemek için basitleştirilmiş bir intrakraniyal anevrizma modeli kullanılmıştır. Anevrizmaya bağlı olarak oluşan sesi belirlemek için, hesaplamalı akışkanlar dinamiği simülasyonları kullanılmış ve iç damar duvarındaki basınç dalgalanmaları incelenmiştir. Kararsız akış basınçlarını bulmak için büyük girdap benzeşimi modelleri kullanılmıştır. Sayısal akış simülasyonlarının sonuçları, anevrizma yakınındaki bölgelerde oluşan ses seviyelerinin arttığını göstermektedir. Anevrizma üzerindeki ses seviyeleri, normal damar çapına sahip bölgelerdeki ses seviyeleri ile karşılaştırıldığında, anevrizmanın ses oluşumunda 10 dB civarında bir artışa neden olduğu görülmektedir. Akış kaynaklı sesteki bu göreceli artışın, ciddi semptomlarla karşılaşmadan önce intrakraniyal anevrizmaların teşhisi açısından önemli olduğu öngörülmektedir.

Anahtar Kelimeler: Akustik basınç, Hesaplamalı akışkanlar dinamiği, Hemodinamik, İntrakraniyal anevrizma

I. INTRODUCTION

Intracranial aneurysm (IA) is the dilatation of the blood vessels in the brain. IA is one of the most critical cardiovascular disorders in the world due to a mortality rate of 50-60% after the aneurysm rupture [1]. IA occurs in various locations in the brain including the sites of bifurcations and sidewalls [2]. The exact mechanism and etiology of the initiation of IA remain unclear; however, it is reported that disturbed hemodynamics play an important role in the alterations of the mechanical behavior of the blood vessel [3]. It is known that there are endothelial cells (ECs) on the blood vessel walls which sense the wall shear stress (WSS) levels generated by the blood flow [4] and orchestrate the growth and remodeling of the blood vessels [5].

WSS is directly related to the friction component of the flow-driven force on the IA wall. Any disturbance in the blood flow affects the blood flow profile inside the vessels and consequently changes the WSS levels. The deteriorated WSS levels on the vessel wall are sensed by ECs and therefore, the growth of the blood vessel is governed by the levels of WSS. If any region on the vessel wall weakens due to the flow-generated effects, then the flow pressure leads to an enlargement of the wall. With the continuous exertion of the excessive flow forces, the enlargement continues to grow and if it exceeds more than 50% of the initial normal diameter of the vessel, surgical intervention can be planned to minimize the risk of IA rupture.

Aneurysms are mainly observed in the aorta and the brain arteries. The aneurysms observed in the aorta have dilated diameters up to 9 cm. In today's clinical practice, if an aortic aneurysm exceeds 5.5 cm, it is accepted with a high risk of rupture [6]. IA has a much smaller diameter since the blood vessels in the brain have diameters in the order of 5 mm. The progression of the IA cannot be detected before facing serious clinical indications and the early diagnosis of the IA is crucial to prevent the further enlargement of the vessel diameter and therefore to reduce the rupture risk.

In the literature, most of the studies related to the IA are about the hemodynamics and rupture mechanisms [7, 8, 9]. There is a lack of studies that investigate sound generation and progression due to the aneurysms. Only a limited number of investigations are focused on the sound generated due to cardiovascular disorders [10, 11, 12].

In this study, the level of sound generated by an IA is investigated by employing the computational fluid dynamics (CFD) approach. An idealized IA geometry is generated for the determination of acoustic pressures on the inner IA surface. The acoustic pressures arise due to the fluctuations of the IA wall pressures. Therefore, the transient and unsteady wall fluctuations are determined using large eddy simulations (LES) and then converted into the frequency domain using fast Fourier transformation (FFT). The obtained acoustic pressure fields provide important information about the sound generated by the IAs, which can be used for the diagnosis of the IAs in the early period.

II. MATERIALS AND METHODS

In this study, a transient flow analysis is performed using the CFD modeling approach. The Fluent package of the ANSYS Workbench 2019 R2 platform is used for modeling and solving the computational flow domain. Due to the fluctuating nature of the inner IA wall pressures, a sound field is generated by the blood flow. Wall pressures are recorded and the FFT algorithm is performed on the recorded pressure values to find the flow-driven sound field. FFT approach is performed using the MATLAB R2017b.

In this section, the details of the numerical model are explained in detail, including the model geometry of the simplified IA, applied CFD methods, and conversion of the results into the frequency domain by employing the FFT approach.

A. MODEL GEOMETRY AND BOUNDARY CONDITIONS

A simplified IA geometry is generated using a nominal blood vessel diameter of 5 mm. In the dilated regions, the maximum diameter of the flow domain reaches 10 mm. The enlarged region of the IA is considered as an ideal sphere with a diameter of 5 mm. In most IA cases, the aneurysm sac is eccentric; therefore, an eccentricity of 2.5 mm is considered between the central line of the blood vessel and the center of the aneurysmal sphere. The simplified IA geometry is generated using the DesignModeler package of the ANSYS Workbench 2019 R2 platform. The three-dimensional (3D) geometry of the simplified IA model is presented in Figure 1. The modeled IA geometry represents an aneurysm with a high risk of rupture.

The focus of the investigation is to determine the generated peak sounds in an aneurysm. The flow-driven sound amplitudes are directly dependent on the flow velocities and the peak sound generation is observed at the instant of peak flow rate [13]. The peak flow velocity reaches up to 1 m/s in the brain arteries [14, 15, 16]. Therefore, the inlet velocity is assigned as 1 m/s to capture the peak sound generation.

In reality, the flow waveform in the brain arteries changes as a function of time due to the pulsatile nature of the cardiovascular system. However, in this study, a quasi-static flow analysis is employed considering a constant inlet velocity of 1 m/s. The reason for using a constant inlet velocity can be explained by the frequencies of the investigated sounds. The heart beat frequency is in the order of 1-2 Hz, but the frequency of the investigated sounds is within the range of 50-600 Hz [11]. In other words, the pulsatile effect in the cardiovascular system is a much slower function compared to the investigated acoustic sound pressure frequencies, which is enabling the investigation of the flow-driven sound generation considering a quasi-static approach.

The outlet boundary is set as a zero-pressure boundary due to the low-pressure levels in the brain arteries [17]. All surfaces except the inlet and outlet boundaries are modeled as rigid walls with no-slip boundary conditions to ensure that the flow velocities are zero at the walls [18].

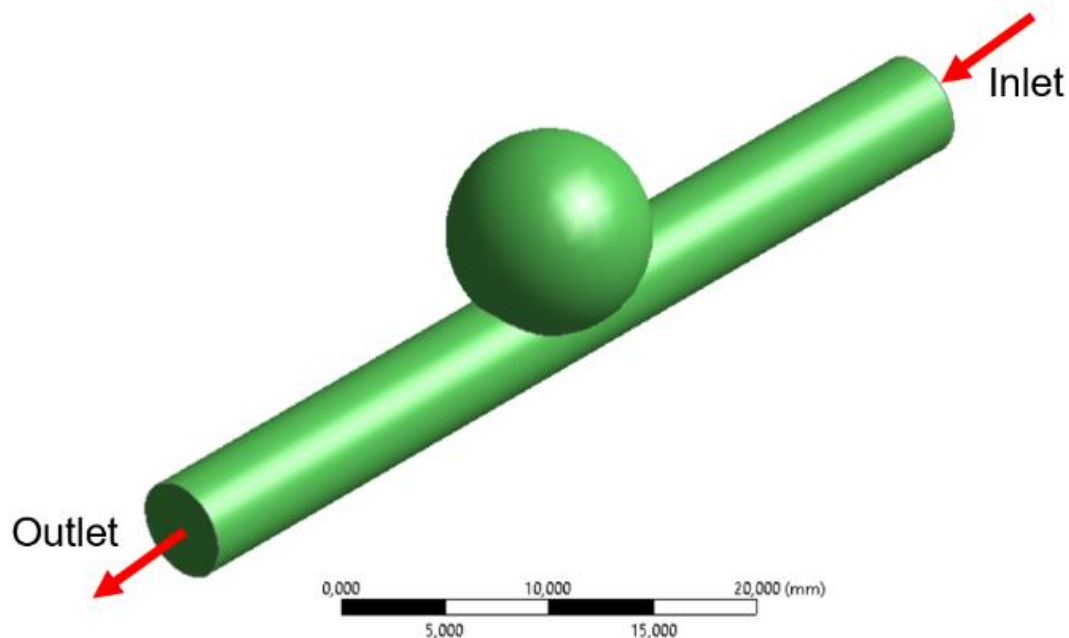


Figure 1. 3D geometry and the boundary conditions of the simplified IA geometry.

B. CFD MODEL

The blood flow inside the IA is simulated using the CFD approach. In CFD methodology, the governing physical equations, known as the Navier-Stokes and continuity equations, are numerically solved by the discretization of space and time. The Navier-Stokes and continuity equations for an incompressible and homogeneous fluid medium are provided in Equation 1 and Equation 2, respectively [19, 20].

$$\rho_f \frac{\partial \mathbf{v}}{\partial t} + \rho_f (\mathbf{v}) \cdot \nabla \mathbf{v} - \nabla \cdot \boldsymbol{\tau}_f = \mathbf{0} \quad (1)$$

$$\nabla \cdot \mathbf{v} = 0 \quad (2)$$

In Equation 1, \mathbf{v} denotes the flow velocity vector; ρ_f denotes the mass density of the blood; t denotes the time; $\boldsymbol{\tau}_f$ denotes the fluid stress tensor which can be described as given in Equation 3.

$$\boldsymbol{\tau}_f = -p\delta_{ij} + 2\mu\varepsilon_{ij} \quad (3)$$

In Equation 3, p denotes the fluid pressure; δ_{ij} denotes the Kronecker delta; μ denotes the dynamic viscosity of the blood; ε_{ij} denotes the strain rate which can be defined as given in Equation 4.

$$\varepsilon_{ij} = \frac{1}{2} (\nabla \mathbf{v} + \nabla \mathbf{v}^T) \quad (4)$$

In this study, the blood is modeled using the Newtonian fluid model with constant viscosity. In reality, the blood has non-Newtonian fluid characteristics where the viscosity changes depending on the shear rate. The non-Newtonian behavior of blood is particularly prominent in small arteries with diameters less than 1 mm. Due to the limited flow area in small arteries, a dynamic shear environment is observed on the arterial wall and this condition leads to a change in the viscosity of the blood depending on the flow conditions. However, this study focuses on a larger aneurysm where the dilated section of the flow reaches 10 mm in diameter. In the large arteries, the shear rate exceeds 50 s^{-1} and nearly constant blood viscosity is observed [21, 22]. Since the flow diameter in the aneurysm sac is large enough, the viscosity of the blood is assumed to be constant and the Newtonian flow behavior is adapted in the fluid model.

The density of the blood is used as $1,060 \text{ kg/m}^3$ [23] and the viscosity is used as 3.5 centipoise (cP) [24]. Since the main interest of the numerical simulations is the fluctuations in the pressure levels on the IA wall, the unsteady flow behavior should be captured accurately. The pressure fluctuations on the aneurysm wall are mainly generated due to the turbulent flow characteristics inside the aneurysm sac. Reynolds averaged Navier-Stokes (RANS) turbulence models are time-averaged methods and they cannot capture the unsteady transient nature of the wall pressure fluctuations.

Detached eddy simulations (DES), large eddy simulations (LES), and direct numerical simulations (DNS) are the methods used for the determination of the unsteady flow characteristics [25]. DES is a hybrid approach that is a combination of RANS and LES models. LES and DNS are more incisive models to determine the pressure fluctuations; however, DNS requires an extremely dense mesh to capture even the tiniest rotating vortices in the flow domain. Therefore, the LES method is adapted in the current numerical simulation due to the adequate solution accuracy and less computational power demand compared to the DNS approach.

A mesh consisting of 1,784,430 tetrahedral elements is employed to perform the LES approach as shown in Figure 2. Five inflation layers are used on the wall to provide accurate boundary layer development. The growth rate between two adjacent inflation layers is set as 1.2. For the regions with nominal artery diameter, the mesh size is employed as 0.45 mm. The mesh density is increased inside the aneurysm sac where the sound is mainly generated. The mesh element sizes on the aneurysm sac are used around 0.075 mm. Patch conforming algorithm is employed as the meshing method.

In total, 6,700 time steps with 0.0001 s increments are used for the flow simulation. A small time step size is required to provide solution convergence. The duration for the completion of the flow simulation is 165 core hours using Intel i7-9750H processor. The results in the first 200 time steps are not used during the post-processing due to the transient effects at the beginning of the flow simulation. The results between 0.02 s and 0.67 s are used to determine the acoustic pressure fluctuations on the IA wall.

C. CONVERSION OF DATA INTO THE FREQUENCY DOMAIN

The results obtained from the flow simulation are in the time domain, which is indicating the change in wall pressures as a function of time. A sample data is provided in Figure 3 for the top point of the IA.

The data in the time domain is required to be converted into the frequency domain to see the spectral behavior of the generated sound field. For this purpose, the FFT algorithm with Hanning windowing is employed using the MATLAB R2017b. After the FFT operation, the results are converted from the time domain to the frequency domain. For smoothing the frequency domain results, the Savitzky-Golay filter, which is available in the MATLAB R2017b toolbox, is applied to the data [26]. After the smoothing of the data, the spectral behavior of the pressure fluctuations can be seen more clearly.

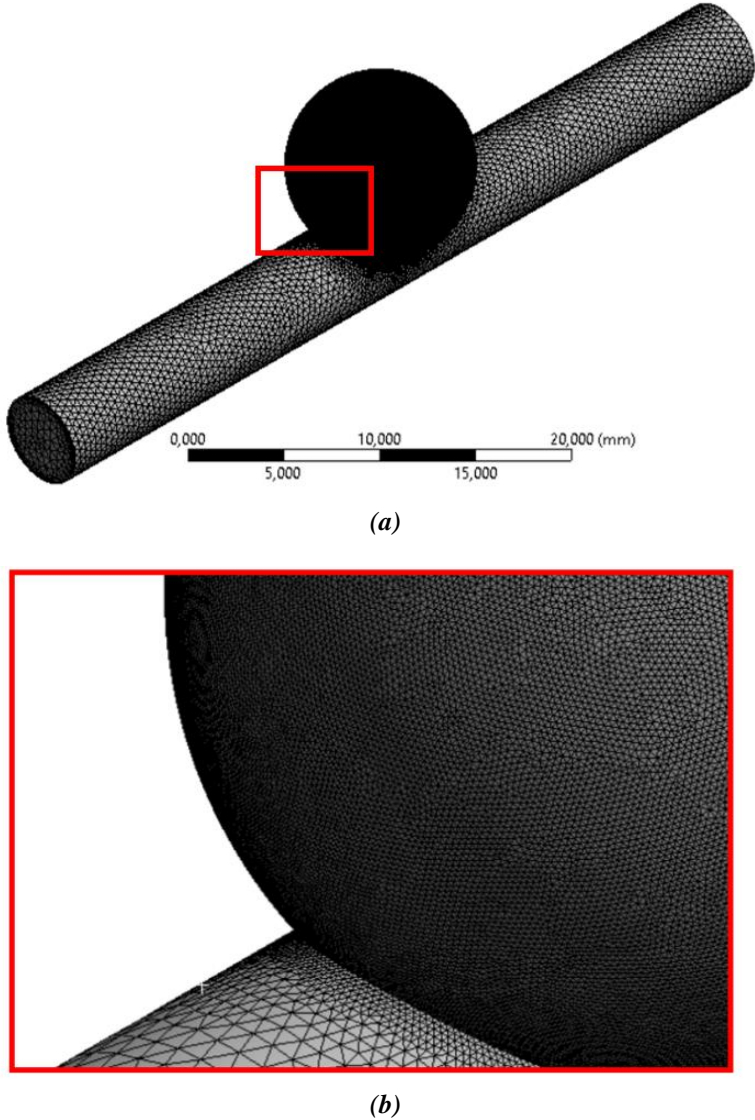
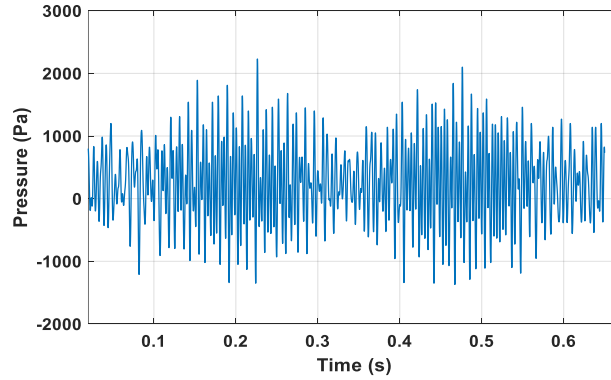
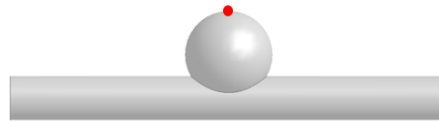


Figure 2. (a) The mesh used for the flow simulation. (b) The red rectangle is zoomed in to clearly show the mesh element sizes.



(a)



(b)

Figure 3. (a) Fluctuating wall pressures at the top of the aneurysm as a function of time. (b) The red point shows the top point of the IA.

In total, 6,500 data points in the time domain are used for the FFT operation to obtain a precise spectral behavior in the frequency domain. In Figure 4, the effect of the number of sample data points is shown by comparing the mean acoustic pressure levels on the top point of the IA. If the number of time-domain data points is less than 4,500, a relative difference of approximately 10% is observed. This indicates that the number of sampling points in FFT should be more than 4,500 to determine an accurate result. When 6,500 data points are used for the FFT, the relative difference becomes lower than 2%, which is considered satisfactory.

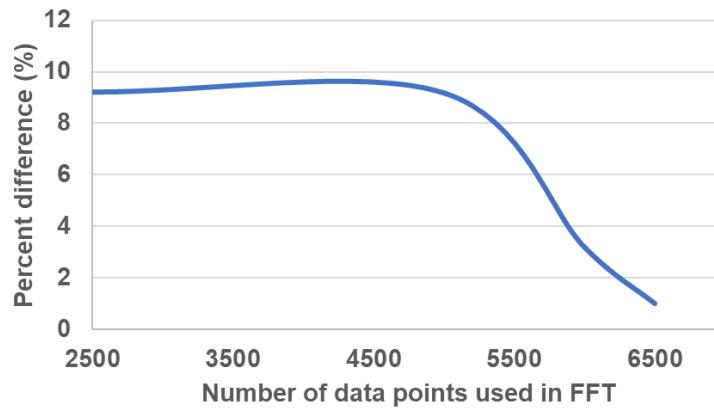


Figure 4. The comparison of mean acoustic pressures on the top point of the IA. As the number of data points in FFT reduces, problematic results are obtained in the frequency domain.

The amplitudes of acoustic pressures in the frequency domain are presented in decibel (dB). Equation 5 is used to convert the pressure amplitudes into dB.

$$p(\text{dB}) = 20 \log_{10} \frac{p(\text{Pa})}{p(\text{Ref})} \quad (5)$$

In Equation 5, $p(\text{dB})$ is the acoustic pressure in dB; $p(\text{Pa})$ is the pressure in Pa; $p(\text{Ref})$ is the reference pressure in Pa, which is used as 1 Pa.

III. RESULTS AND DISCUSSION

In this section, the fluctuating wall pressures are investigated in the frequency domain to observe the acoustic effects of the IA. Since there is a stiff skull in the head, it acts as a sound barrier, and the flow-generated acoustic effects can be transmitted through the brain tissues and reach the eyes. Therefore, the vibration measurements on the eyes can provide important information for the diagnosis of abnormal flow conditions in the brain arteries.

The fluctuating wall pressures, called acoustic pressures, are determined at several locations of the IA wall. The time-domain results provided in Figure 3 show that there are two complete waves within the range of 0.1-0.6 s. This indicates that there is a repeated circulation inside the aneurysm sac, which repeats itself about every 0.25 seconds.

In Figure 5, the velocity contour plot is provided for various instants on the central cross-sectional plane of the flow domain. Since the mainstream velocity is nearly constant during the flow analysis, only the flow contours in the aneurysm sac are investigated in Figure 5. It is seen that the mainstream flow velocity is much higher compared to the circulating flow in the IA and the central site of the aneurysm is nearly stagnant [17, 18, 27]. The flow velocity fluctuates with time and results in the IA wall pressure fluctuations. The peak flow velocity on the aneurysm wall reaches up to 0.3 m/s [18].

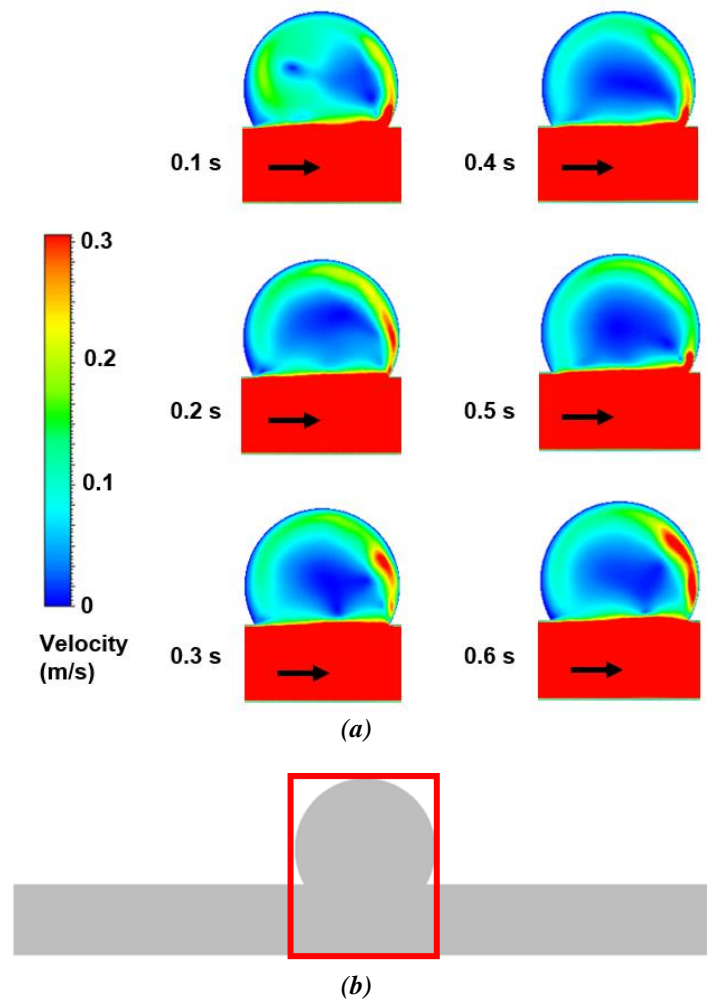


Figure 5. (a) Velocity contour plots for various instants on the cross-sectional plane of the aneurysmal site. The velocity contour plots are shown at 0.1 s, 0.2 s, 0.3 s, 0.4 s, 0.5 s, and 0.6 s. The black arrows in the mainstream show the flow direction. (b) The red rectangle at the bottom plot shows the region of interest for the colored contour velocity plots.

The fluctuating behavior of the flow can also be seen in the WSS levels as shown in Figure 6. The turbulent activity inside the aneurysm sac leads to varying shear stress levels on the wall. These results also indicate that the LES flow solver employed in the flow simulation is capable to determine the unsteady behavior of the flow variables. It is observed that the WSS levels on the IA are quite lower compared to the regions close to the mainstream flow [17, 18]. Most of the IA sacs experience a WSS level lower than 1 Pa due to the small flow velocities in the aneurysm sac. The maximum WSS level on the IA wall is approximately 5 Pa. The regions close to the mainstream flow are exposed to a high shear environment which is higher than 5 Pa [18].

In Figure 7, the FFT results of several points on the IA wall are presented. Eight different points on the top wall are used to obtain the color-coded acoustic pressure map. The colored plot in Figure 7 shows the amplitudes of the acoustic pressures in dB as a function of the frequency and the location on the IA wall. It is observed that the highest activity in terms of sound generation is seen within the frequency range of 50-300 Hz. For frequencies higher than 300 Hz, acoustic pressures tend to decrease significantly [10, 28]. Acoustic pressure amplitudes gradually decrease as the frequency increases [13]. When the points which are close and distant to the aneurysm sac are compared, it can be concluded that the highest sound is generated on the points close to the IA. This indicates that the presence of IA leads to an excessive sound generation compared to the blood vessels with normal diameter. There is a reduction in the acoustic pressure generation with the increasing distance to the aneurysm. There is a general decrease in acoustic pressures at all frequencies as the distance to the IA increases [28].

There is an important difference in the amplitudes of the acoustic pressures within 450-800 Hz between the points distant from the IA and the points on the IA. The acoustic pressure amplitudes are relatively higher within 450-850 Hz for the points on the IA wall. It is concluded that the acoustic pressure amplitudes at high frequencies (between 450 Hz and 850 Hz) can also indicate the presence of IA based on the relatively increased fluctuating pressure amplitudes.

In Figure 8, the FFT results of two points are compared to see the difference between a point on the IA and a point distant from the IA. For a point on the IA, the highest acoustic generation is observed with a peak value of approximately 25 dB. There is a dominant peak acoustic pressure value of around 150 Hz. After passing 300 Hz, acoustic pressure amplitudes decrease significantly as previously observed in Figure 7. Another peak value is observed around 500 Hz. After this peak, the amplitudes gradually decrease with the increasing frequency and acoustic pressure amplitudes become negligible at around 1,000 Hz with a value of around -20 dB. FFT results of the two points presented in Figure 8 are similar in terms of the general behavior because the peaks are observed at the same frequencies for both of the points. The main difference between the two points is related to the amplitudes of the acoustic pressures. Approximately 10 dB of acoustic pressure amplitude difference is observed between a point on the IA and a point distant from the IA. From this comparison, it can be concluded that the presence of IA in the brain can result in 10 dB increased flow-driven sound generation. This excessive sound is transmitted through the soft tissues in the brain and the IA-driven acoustic effect can be detected by the measurements performed on the eye surfaces.

The propagation of the excessive sound generated by the IA in the brain is aimed to be investigated in future studies to determine the feasibility of the detection of the IA through the vibration measurements performed on the eyes. The skull cannot be used for effective sound measurement, but the eyes can be used for vibroacoustic measurements due to their soft structural material properties [29].

This study has some limitations. A more complicated mesh that includes more than 10 million mesh elements can better predict the unsteady nature of the pressure fluctuations on the wall. The IA geometry used in the study is a primitive geometric model, and the same computational methodology can be applied to a realistic IA geometry, which can be determined using clinical measurements and medical imaging techniques such as magnetic resonance imaging (MRI) and computed tomography (CT). The inlet flow is kept constant by considering a quasi-steady approach, but this method can be improved by using a time-dependent transient flow waveform at the inlet boundary of the flow domain. The Newtonian blood model used in this study can be improved by employing non-Newtonian blood models

which consider the change in the blood viscosity depending on the shear environment [30]. Nevertheless, the applied methodology in this study achieved to numerically determine the acoustic pressures on the IA wall and provided an important insight to understand the sound generation from an aneurysm.

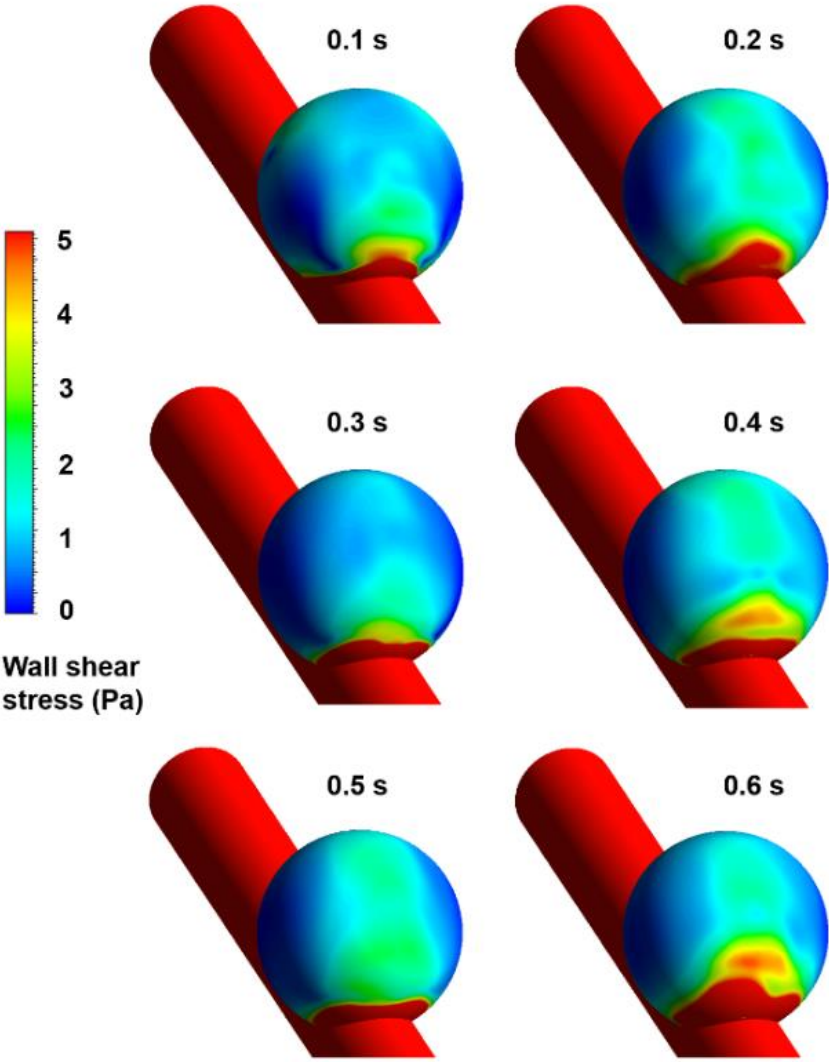
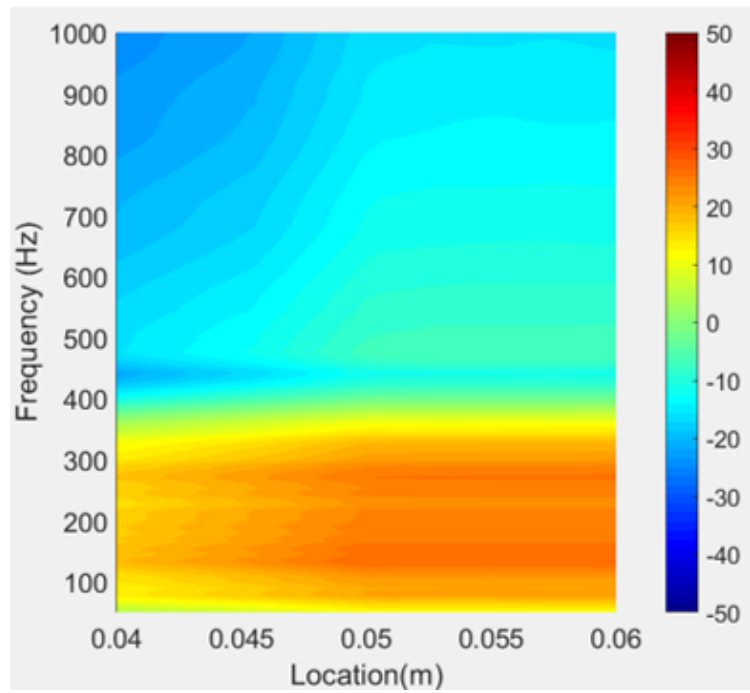
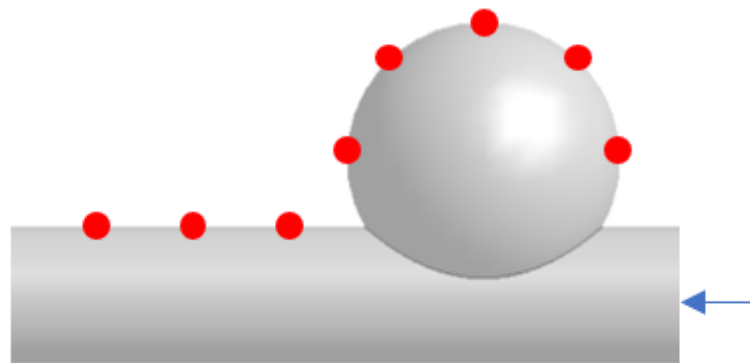


Figure 6. Wall shear stress distribution on the IA sac for various instants.

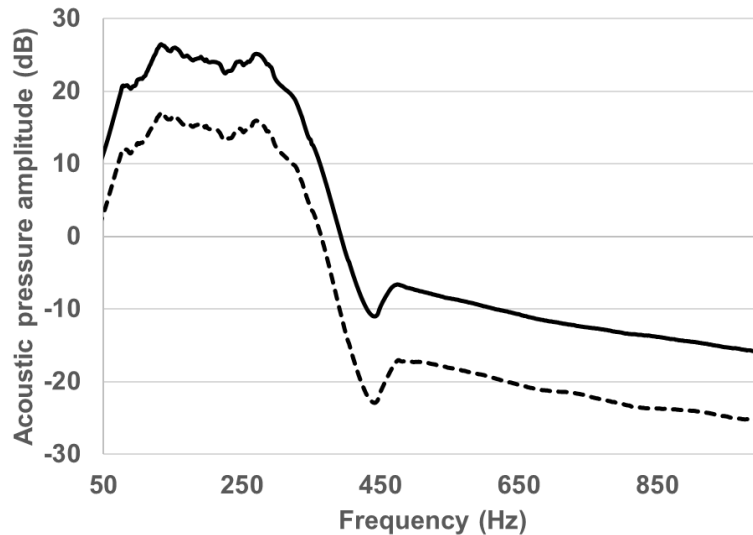


(a)

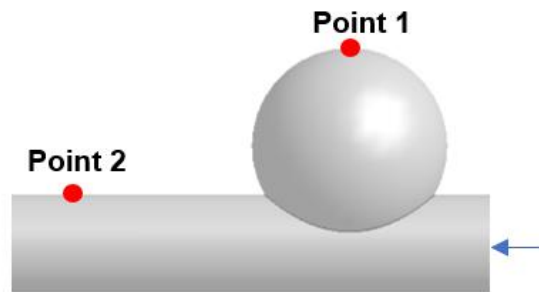


(b)

Figure 7. (a) Acoustic pressures (dB) on the IA wall. The color-coded contour plot shows the amplitudes (dB) of the acoustic pressures as a function of frequency and location. The red points are the locations of the data measurements within the location range of 0.040 and 0.060 m. (b) There are 8 measurement points corresponding to the locations of 0.040, 0.043, 0.046, 0.049, 0.051, 0.054, 0.057, and 0.060 m. The blue arrow shows the flow direction.



(a)



(b)

Figure 8. (a) Comparison of the acoustic pressures between Point 1 (solid line) and Point 2 (dashed line). (b) The locations of Point 1 and Point 2. The blue arrow shows the flow direction.

IV. CONCLUSION

Aneurysms in the brain are life-threatening health disorders. An eventual rupture of IA can result in adult disability or even death. The growth of an IA progresses silently and it is difficult to diagnose an IA before observing clinical symptoms. Therefore, it is critical to develop a non-invasive diagnostic tool that can be used to detect IA at an early stage. Depending on the constriction or expansion of the blood vessels, abnormal sounds in the body may indicate serious medical conditions.

In this study, the aneurysm-driven sounds in the brain are investigated from a diagnostic perspective. For this purpose, the fluctuating pressures on the IA wall are numerically modeled using CFD methodology to understand the sound generation from an aneurysm in the brain. A simplified IA geometry is employed in the flow simulations with a nominal diameter of 5 mm and dilated diameter of 10 mm. For the flow solver, the LES approach is adapted to determine the unsteady behavior of the blood flow-driven wall pressures. The numerically determined IA wall pressure levels are determined in the time domain. The determined pressure levels in the time domain are converted into the frequency domain using the FFT algorithm with Hanning windowing and Savitzky-Golay filtering.

The obtained results in the frequency domain showed that the flow-driven acoustic pressures at the proximity of the aneurysmal site are higher compared to the points distant from the aneurysm. In the presence of an IA in the brain, an increase in acoustic pressure amplitude of around 10 dB is observed.

This shows that an aneurysm acts as a sound source and leads to relatively increased acoustic pressure levels around the aneurysm site. The relatively increased sound levels can be evaluated as an early sign of an IA formation, and preventive precautions can be taken before facing serious symptoms. Since the skull is a stiff material, it acts as an acoustic barrier. Therefore, the eyes can be used for the measurement of sound and vibration to decide on the presence of IA in the brain. In future studies, it is aimed to investigate the feasibility of measuring vibroacoustic effects on the eyes for the assessment of IA in the brain.

ACKNOWLEDGEMENTS: This study is funded by TÜBİTAK (The Scientific and Technological Research Council of Türkiye) 3501 – Career Development Program (Project number: 221M001).

V. REFERENCES

- [1] P. S. Amenta, S. Yadla, P. G. Campbell, M. G. Maltenfort, S. Dey, S. Ghosh, M. S. Ali, J. I. Jallo, S. I. Tjournakaris, L. F. Gonzalez, A. S. Dumont, R. H. Rosenwasser and P. M. Jabbour, “Analysis of nonmodifiable risk factors for intracranial aneurysm rupture in a large, retrospective cohort,” *Neurosurgery*, vol. 70, no. 1, pp. 693–701, 2012.
- [2] H. Asgharzadeh, H. Asadi, H. Meng and I. Borazjani, “A non-dimensional parameter for classification of the flow in intracranial aneurysms. II. Patient-specific geometries,” *Physics of Fluids*, vol. 31, no. 3, p. 031905, 2019.
- [3] J. J. Chiu and S. Chien, “Effects of disturbed flow on vascular endothelium: pathophysiological basis and clinical perspectives,” *Physiological Reviews*, vol. 91, no. 1, pp. 327–387, 2011.
- [4] J. D. Humphrey, “Vascular adaptation and mechanical homeostasis at tissue, cellular, and sub-cellular levels,” *Cell Biochemistry and Biophysics*, vol. 50, no. 2, pp. 53–78, 2008.
- [5] J. M. Dolan, J. Kolega and H. Meng, “High wall shear stress and spatial gradients in vascular pathology: a review,” *Annals of Biomedical Engineering*, vol. 41, no. 7, pp. 1411–1427, 2013.
- [6] H. E. Salman, B. Ramazanli, M. M. Yavuz and H. C. Yalcin, “Biomechanical investigation of disturbed hemodynamics-induced tissue degeneration in abdominal aortic aneurysms using computational and experimental techniques,” *Frontiers in Bioengineering and Biotechnology*, vol. 7, no. 111, 2019.
- [7] J. C. Lasheras, “The biomechanics of arterial aneurysms,” *Annual Review of Fluid Mechanics*, vol. 39, no. 1, pp. 293–319, 2007.
- [8] D. M. Sforza, C. M. Putman and J. R. Cebal, “Hemodynamics of cerebral aneurysms,” *Annual Review of Fluid Mechanics*, vol. 41, no. 1, pp. 91–107, 2009.
- [9] T. Hassan, E. V. Timofeev, M. Ezura, T. Saito, A. Takahashi, K. Takayama and T. Yoshimoto, “Hemodynamic analysis of an adult vein of Galen aneurysm malformation by use of 3D image-based computational fluid dynamics,” *American Journal of Neuroradiology*, vol. 24, no. 6, pp. 1075–1082, 2003.
- [10] H. E. Salman and Y. Yazicioglu, “Flow-induced vibration of constricted artery models with surrounding soft tissue,” *The Journal of the Acoustical Society of America*, vol. 142, no. 4, pp. 1913–1925, 2017.

- [11] H. E. Salman, C. Sert and Y. Yazicioglu, “Computational analysis of high frequency fluid-structure interactions in constricted flow.” *Computers & Structures*, vol. 122, pp. 145–154, 2013.
- [12] K. Ozden, C. Sert and Y. Yazicioglu, “Numerical investigation of wall pressure fluctuations downstream of concentric and eccentric blunt stenosis models,” *Proceedings of the Institution of Mechanical Engineers, Part H: Journal of Engineering in Medicine*, vol. 234, no. 1, pp. 48–60, 2020.
- [13] A. O. Borisjuk, “Modeling of noise generation by a vascular stenosis,” *International Journal of Fluid Mechanics Research*, vol. 29, no. 1, pp. 65–88, 2002.
- [14] H. Asgharzadeh and I. Borazjani, “Effects of Reynolds and Womersley numbers on the hemodynamics of intracranial aneurysms,” *Computational and Mathematical Methods in Medicine*, vol. 2016, 2016.
- [15] K. M. Saqr, S. Rashad, S. Tupin, K. Niizuma, T. Hassan, T. Tominaga and M. Ohta, “What does computational fluid dynamics tell us about intracranial aneurysms? A meta-analysis and critical review,” *Journal of Cerebral Blood Flow & Metabolism*, vol. 40, no. 5, pp. 1021–1039, 2020.
- [16] H. Asgharzadeh, H. Asadi, H. Meng and I. Borazjani, “A non-dimensional parameter for classification of the flow in intracranial aneurysms. II. Patient-specific geometries,” *Physics of Fluids*, vol 31, no. 3, p. 031905, 2019.
- [17] M. R. Levitt, M. C. Barbour, S. R. du Roscoat, C. Geindreau, V. K. Chivukula, P. M. McGah, J. D. Nerva, R. P. Morton, L. J. Kim and A. Aliseda, “Computational fluid dynamics of cerebral aneurysm coiling using high-resolution and high-energy synchrotron X-ray microtomography: comparison with the homogeneous porous medium approach,” *Journal of Neurointerventional Surgery*, vol. 9, no. 8, pp. 777–782, 2017.
- [18] J. R. Cebal, F. Mut, D. Sforza, R. Löhner, E. Scrivano, P. Lylyk and C. M. Putman, “Clinical application of image-based CFD for cerebral aneurysms,” *International Journal for Numerical Methods in Biomedical Engineering*, vol. 27, no. 7, pp. 977–992, 2011.
- [19] H. Zhang, X. Zhang, S. Ji, Y. Guo, G. Ledezma, N. Elabbasi and H. deCougny, “Recent development of fluid–structure interaction capabilities in the ADINA system,” *Computers & Structures*, vol. 81, no. 8-11, pp. 1071–1085, 2003.
- [20] C. M. Scotti and E. A. Finol, “Compliant biomechanics of abdominal aortic aneurysms: a fluid–structure interaction study,” *Computers & Structures*, vol. 85, no. 11–14, pp. 1097–1113, 2007.
- [21] D. F. Young, “Fluid mechanics of arterial stenoses,” *Journal of Biomechanical Engineering*, vol. 101, no. 3, pp. 157–175, 1979.
- [22] A. Arzani, “Accounting for residence-time in blood rheology models: do we really need non-Newtonian blood flow modelling in large arteries?,” *Journal of the Royal Society Interface*, vol. 15, no. 146, p. 20180486, 2018.
- [23] M. C. Brindise, M. M. Busse and P. P. Vlachos, “Density-and viscosity-matched Newtonian and non-Newtonian blood-analog solutions with PDMS refractive index,” *Experiments in Fluids*, vol. 59, no. 11, pp. 1–8, 2018.
- [24] T. G. Papaioannou and C. Stefanadis, “Vascular wall shear stress: basic principles and methods,” *Hellenic Journal of Cardiology*, vol. 46, no. 1, pp. 9–15, 2005.
- [25] M. M. Molla and M. C. Paul, “LES of non-Newtonian physiological blood flow in a model of arterial stenosis,” *Medical Engineering & Physics*, vol. 34, no. 8, pp. 1079–1087, 2012.

- [26] S. R. Krishnan and C. S. Seelamantula, "On the selection of optimum Savitzky-Golay filters," *IEEE Transactions on Signal Processing*, vol. 61, no. 2, pp. 380–391, 2012.
- [27] L. Liang, D. A. Steinman, O. Brina, C. Chnafa, N. M. Cancelliere and V. M. Pereira, "Towards the clinical utility of CFD for assessment of intracranial aneurysm rupture – a systematic review and novel parameter-ranking tool," *Journal of Neurointerventional Surgery*, vol. 11, no. 2, pp. 153–158, 2019.
- [28] T. D. Mast and A. D. Pierce, "A theory of aneurysm sounds," *Journal of Biomechanics*, vol. 28, no. 9, pp. 1043–1053, 1995.
- [29] J. Hasegawa and K. Kobayashi, "Blood flow noise transducer for detecting intracranial vascular deformations," *Acoustical Science and Technology*, vol. 22, no. 1, pp. 5–11, 2001.
- [30] J. Bernsdorf and D. Wang, "Non-Newtonian blood flow simulation in cerebral aneurysms," *Computers & Mathematics with Applications*, vol. 58, no. 5, pp. 1024–1029, 2009.